ELECTRON OMNIDIRECTIONAL INTENSITY CONTOURS IN THE EARTH'S OUTER RADIATION ZONE AT THE MAGNETIC EQUATOR*

by

H. D. Owens and L. A. Frank

Department of Physics and Astronomy
University of Iowa
Iowa City, Iowa

July 1967

*Research supported in part by the National Aeronautics and Space Administration under Grant NsG-233-62.

ABSTRACT

A comprehensive graphic display of the omnidirectional intensities of electrons (E > 40 keV, > 230 keV, and > 1.6 MeV) in the outer radiation zone observed during the ten-month period October 1962 through July 1963 with an array of Geiger-Mueller tubes borne on the earth-satellite Explorer 14 is presented. The observations are displayed as contours of constant omnidirectional intensities of electrons with energies exceeding the above thresholds as functions of shell-parameter L and time at the magnetic equator. Although many of the phenomena apparent in these maps of outer zone electron intensities have previously been discussed, the present graphic summary provides an extensive panorama of the morphology of the energetic electron distributions in the outer zone and a compact, concise medium for comparison with related ground-based and satellite measurements of geophysical phenomena.

I. INTRODUCTION

In 1958 large intensities of energetic charged particles trapped within the earth's magnetic field were detected at altitudes exceeding several hundred kilometers above the earth's surface. These initial observations were acquired with satellites having relatively short lifetimes. Identification and detailed study of the sources and of the loss mechanisms for charged particles in the earth's radiation zones requires observations spanning periods of weeks and months; increasing use of the earth-satellite as an observational tool has made it possible to obtain many comprehensive measurements of the radiation environment in the vicinity of the earth [cf McIlwain, 1963; Frank, 1965a; Frank, Van Allen and Hills, 1964; Davis, 1965; Freden, Blake and Paulikas, 1965; Gabbe and Brown, 1966; Vette, 1966] since the initial surveys in these regions.

Over a period of approximately ten months of almost continuous operation the University of Iowa array of Geiger-Mueller tubes on the Explorer 14 satellite provided over 50,000 individual measurements of the charged particle intensities in the outer radiation zone near the magnetic equator. Via utilization of selected segments of these observations, other authors have investigated numerous features of the distributions and temporal variations of outer zone electron

intensities [e.g., Frank, Van Allen, Whelpley, and Craven, 1963; Frank, Van Allen, and Hills, 1964; Frank, 1965a, b, c]. Our present task, however, is directed toward further organization of the observations of electron intensities in the outer radiation zone obtained with Explorer 14 over the period October 1962 through July 1963 in order to provide an extensive panorama of the morphology of the electron intensities and a compact medium for future comparisons with related ground-based and satellite observations of geophysical phenomena.

II. DESCRIPTION OF INSTRUMENTATION

The Explorer 14 satellite was launched on 2 October 1962, and transmitted data from launch through 8 August 1963. Temporary failure of the satellite telemetry system occurred during late January. Post-launch orbital parameters and methods of data acquisition and reduction have been discussed elsewhere [Frank, Van Allen, Whelpley, and Craven, 1963; Frank, Van Allen, and Hills, 1964; Frank, 1965a]. Several items of particular importance to this study may, however, be reviewed.

At launch the local time of the satellite apogee position at 16.4 R_E geocentric radial distance was approximately 07:30. Perigee altitude was at 281 kilometers and the orbital inclination and period were 33° and 36.4 hours, respectively. The spacecraft was spin-stabilized (initially with a spin frequency ~ 15 r.p.m.) with the axes of the conical fields of view of the University of Iowa detectors directed perpendicular to the spin axis; at launch the angle between the line directed along this spin axis and the line from the satellite to the sun was approximately 150°. The response of each G.M. tube was accumulated over a period of 10.24 seconds, or over two spin periods of the spacecraft during the period immediately following launch, and subsequently telemetered. The University of Iowa complement of detectors

borne on Explorer 14 featured four Geiger-Mueller tubes, designated as the 213A, 213B, 213C and the 302 G.M. tubes. Geometric factors and threshold energies for these G.M. tubes are given in Table I.

TABLE I

Characteristics of the University of Iowa Detectors on Explorer 14*

Omnidirectional				Directional		
Detector	Shielding	Penetrating Particles	Geometric Factor, G, (cm^2)	Shielding	Penetrating Particles	Geometric Factor, g, (cm^2-sr)
213A	Side shielding: 4.4 g/cm^2 Pb	Protons $\geq$ 70 MeV	0.2	1.2 mg/cm^2 mica	Protons $\geq$ 500 keV Electrons $\geq$ 40 keV	2×10^{-3}
213B	0.55 g/cm^2 Mg	Electrons $\gtrsim$ 10 MeV	0.2	48 mg/cm^2 Al	Protons $\geq$ 4.5 MeV Electrons $\geq$ 230 keV	2×10^{-3}
213C			0.2	1.2 mg/cm^2 mica plus sweeping magnet	Protons $\geq$ 500 keV Electrons $\geq$ 200 keV	3×10^{-3}
302	265 mg/cm^2 Mg. 400 mg/cm^2 stainless steel	Protons $\geq$ 23 MeV Electrons $\gtrsim$ 1.6 MeV	0.6	- - -	- - -	- - -

*See also Frank, Van Allen and Hills [1964]

III. TREATMENT OF THE OBSERVATIONS

The University of Iowa Explorer 14 observations which were available for the present analysis are in the form of a master data tape compiled at the University of Iowa Computer Center. This tape provides the telemetered responses of the four Geiger-Mueller detectors (in units of counts $(\text{sec})^{-1}$) accompanied with the following information as functions of Universal Time (U.T.): local time, geocentric radial distance, right ascension and declination, B and L, geomagnetic latitude, and geographic longitude of the satellite position. Three adjustments have been applied to these observations in the course of this analysis and are described here.

A. The R(r) correction

The first correction applied to the telemetered responses of the Geiger-Mueller tubes is the "dead-time" correction. This correction arises from the inability of the G.M. tube to resolve near-coincidental particles penetrating the active volume of the detector, and in practice is significant for responses exceeding $\sim 4{,}000$ counts $(\text{sec})^{-1}$. The dependence of the true counting rate R on the apparent, or telemetered, counting rate r was determined in the laboratory prior to launch for each G.M. tube. The functions R(r) were approximated with polynomials.

The errors introduced by the use of the polynomial approximations were < 15% over the range of the apparent counting rates included in the present study.

B. The B/B_o Normalization

The satellite trajectory intersects L-shells over a range of B/B_o-values (or magnetic latitudes λ_m), and hence a second adjustment for magnetic latitude of the observation is necessary in order to effectively separate the temporal variations in electron intensities from the B/B_o dependence at a specified L-value. To accomplish this, the nature of the B/B_o dependences of the spin-averaged responses of the G.M. tubes was established via graphs similar to that shown in Figure 1. Observations from each of the consecutive inbound and outbound intersections of an orbit with a L-shell are connected by straight lines. Figure 1 shows the responses of one of the G.M. tubes, 213B, as functions of B/B_o along a given L-shell. The responses of each detector were grouped into monthly intervals and plotted at L-values of 4, 5, 6, and 7. The average B/B_o dependences of detector responses as functions of L for each month were determined from sets of observations such as those displayed in Figure 1. Linear interpolation was invoked in order to provide the latitude dependences of the responses at intermediate L-values; linear extrapolation was used for $L > 7$ and $L < 4$. The latitude dependences of the detector responses were

approximated by

$$R_{xo} = R_{xl}\left(\frac{B}{B_o}\right)^{-(\alpha_x L + \beta_x)}, \quad \alpha_x L + \beta_x < 0,$$

where R_{xl} is the detector response in true counts$(\text{sec})^{-1}$ at given B/B_o and L, the subscript x is A, B, C, or D corresponding to the 213A, 213B, 213C or 302 G.M. tubes, respectively, and R_{xo} is the detector response at the magnetic equator. All observations presented here were normalized to the magnetic equator via the above relationship.

C. Calculation of G.M. Tube Efficiencies as Functions of Spectral Index n

Three of the Explorer 14 Geiger-Mueller tubes were directional detectors. Frank, et al [1964] have shown that if $\bar{j}$ is the spin-averaged directional intensity, then the omnidirectional intensity of electrons with energies greater than the nominal threshold energy E_T, $J_o(> E_T)$, is given within a factor of two for typical angular distributions of outer zone electron intensities by

$$J_o(> E_T) = 10\ \bar{j}\ (> E_T),$$

where

$$\bar{j}\ (> E_T) = R/\epsilon g.$$

If R is the response of the omnidirectional 302 G.M. tube, then the omnidirectional intensity is

$$J_o(> E_T) = R/\epsilon G,$$

where R above are the corresponding responses of the G.M. tubes in true counts $(sec)^{-1}$ and g (or G) is the directional (or omnidirectional) geometric factor listed in Table 1. The efficiency ϵ depends upon the efficiency of the Geiger-Mueller tube for counting monoenergetic electrons, ϵ (E), as a function of electron energy and on the electron spectrum being sampled. The Geiger-Mueller tube efficiencies for counting monoenergetic electrons are steep functions of electron energy in the energy ranges bracketing their assigned nominal threshold energies, E_T. If the electron integral spectrum is approximated by a power law, E^{-n}, and an intermediate threshold energy, E_T', is assigned which assumes a step-function efficiency profile as a function of electron energy such that the efficiency $\epsilon'(< E_T') = 0$ and $\epsilon'(> E_T') = 1$, then E_T' is, by definition, found by solving the integral relation

$$\int_0^\infty \frac{dJ_o}{dE} \epsilon\ (E)\ dE = \int_{E_T'}^\infty \frac{dJ_o}{dE} \epsilon'\ (E)\ dE\ ,$$

where ϵ (E) is the measured efficiency of the Geiger-Mueller tubes for counting electrons of energy E, and $\frac{dJ_o}{dE}$ is the electron differential energy spectrum. Clearly E_T' is dependent upon the spectral index n,

and

$$J_o(> E_T) = (E_T/E_T')^{-n} J_o(> E_T').$$

The quantity E_T' was calculated using, in turn, the efficiencies of the 213B and 302 G.M. tubes for counting monoenergetic electrons as determined with laboratory electron accelerators and spectrometers. Relations for the dependences of the calculated E_T'-values upon n were then derived for the 213B G.M. tube

$$E_T'(213B) = 6.125 \times 10^5 - 2.975 \times 10^4 \ (n-3) \text{ eV},$$

and the 302 G.M. tube

$$E_T'(302) = 3.065 \times 10^6 - 1.325 \times 10^5 \ (n-4) \text{ eV}.$$

In the present calculations n was approximated with the zero-order iteration of the counting rates and nominal threshold energies of the detectors,

$$n = \frac{\log\left(J_o(> 230 \text{ keV})\right) - \log\left(J_o(> 1.6 \text{ MeV})\right)}{\log(1.6) - \log(0.23)}$$

$$= \frac{\log(10\ R_B/g_B) - \log(R_D/G_D)}{0.842}.$$

The omnidirectional integral intensity of electrons with energies greater than E_T becomes

$$J_o(> 230 \text{ keV}) = 10\ R_B/\epsilon_B g_B,$$

and

$$J_o(> 1.6 \text{ MeV}) = R_D/\epsilon_D G_D,$$

where R_B and R_D are the responses of the 213B and the 302 Geiger-Mueller tubes, respectively, in units of true counts$(sec)^{-1}$, and $\epsilon_B g_B$ and $\epsilon_D G_D$ have been approximated by

$$\log (\epsilon_B g_B) \simeq - 0.420\ n - 2.700 \quad \text{and}$$

$$\log (\epsilon_D G_D) \simeq - 0.288\ n - 0.222\ .$$

The substitution of these approximations for the more complex exact relationships facilitated comparison of manual calculation with computer output without a significant loss in accuracy. The unshielded 213A G.M. tube is assumed, with adequate accuracy, to be an ideal threshold detector; hence the above calculations were not necessary in order to compute electron ($E > 40$ keV) omnidirectional intensities from the spin-averaged responses of this G.M. tube. The proton contributions to the responses of the 213B and 302 G.M. tubes have been assumed to be negligible for the L-value range $3.5 \leq L \leq 8.0$ [cf. Frank, Van Allen and Hills, 1964]; and the usually negligible proton contributions to the responses of the 213A G.M. tube were subtracted by utilizing the responses of the 213C G.M. tube (see Table I).

The effect that these B/B_o and "$\epsilon(n)$" adjustments described above have on a selected segment of the observations is summarized in Figure 2. Of interest are the instances in which measurements were available from both an inbound and outbound pass on a particular day. Any dependence of the detector (in this case 213B) responses

upon B/B_o is reflected in a separation of the inbound and outbound responses along the vertical axis. For the time period covered in Figure 2 observations during such inbound and outbound passes always differed in B/B_o. At L = 4.2 the present normalization of omnidirectional intensities to $\lambda_m = 0°$ is adequate; at L = 6.0, however, this normalization is less effective but remains adequate for our present purposes. The "$\epsilon(n)$" correction is important during the initial stages of a geomagnetic storm.

IV. OBSERVATIONS

Contours of constant intensity as functions of L and time for omnidirectional intensities of electrons (E > 40 keV, E > 230 keV and E > 1.6 MeV) at the geomagnetic equator for the ten-month period October 1962 through July 1963 are shown in Figures 3, 4, 5, 6 and 7. These curves summarize the observations after being subjected to the "R(r)", the B/B_o and the "ϵ(n)" adjustments previously discussed. The B/B_o correction is essential to eliminate the dependence of the omnidirectional intensities on the magnetic latitude of the satellite position. The "ϵ(n)" correction is a relatively small correction (refer to Figure 2). Each contour in Figures 3 through 7 is assigned an omnidirectional intensity of 1, 2, 5, or 7 times a power of 10. A contour encloses the number which designates its intensity. All the contours lying above L = 7.0 or below L = 4.0 are dashed as the slope of the B/B_o graphs was not calculated directly, but extrapolated, for these regions. The contours for electron (E > 40 keV and > 230 keV) omnidirectional intensities shown in Figure 7 for the period June through July 1963 are heavily dashed in order to designate that errors in calculating intensities from spin-averaged directional detector responses amounting to $\sim$ 40% are probable due to a low spin rate ($\lesssim$ 2 r.p.m.) of the spacecraft during this period. Frank has shown

[1965a, 1965b] that for $L \gtrsim 6$ there exists a significant local-time dependence for electron ($E > 40$ keV and > 1.6 MeV) intensities. The effect is quite pronounced at $L = 8$. No local-time correction has been applied to these data. The local time of the position of the satellite apogee was near local midnight during late-January 1963 and near local noon during late-July 1963. Gross temporal variations of the intensities presented in Figures 3 through 7 are assumed to be of duration greater than or equal to the orbital period of the spacecraft. In general, however, a level of intensity exists for several days. Although this assumption concerning the overall time-scale of the intensity variations appears to be generally justified with the principal exception of the periods encompassing the onsets of geomagnetic storms, Frank [1965a] has reported a large-scale depletion occurring within a time period of 1/4 to 1/2 hour. This relatively rare event was apparent in the intensities of electrons ($E > 40$ keV, > 230 keV and > 1.6 MeV). This event is not reflected in the contours, and is cited as an example of the limitation of this form of presentation.

Typical omnidirectional intensities of electrons ($E > 40$ keV, > 230 keV and > 1.6 MeV) are available after cursory examination of Figures 3, 4, 5, 6 and 7. Quiet-time electron ($E > 40$ keV) intensities of $\sim 2 \times 10^7$ $(cm^2\text{-sec})^{-1}$ are contrasted with those of more active periods, as indicated by relatively high daily sum K_p, of $\sim 10^8$ $(cm^2\text{-sec})^{-1}$. The peak omnidirectional intensities of electrons

($E > 230$ keV) are typically 5×10^6 $(cm^2\text{-sec})^{-1}$ during times characterized by low K_p daily sums, and $\sim 2 \times 10^7$ $(cm^2\text{-sec})^{-1}$ during disturbed periods with a high K_p daily sum. The quiet-time omnidirectional intensities of electrons ($E > 1.6$ MeV) are typically $\sim 10^5$ $(cm^2\text{-sec})^{-1}$ at $L \simeq 4.5$. Geomagnetically active periods are characterized by peak electron ($E > 1.6$ MeV) intensities $\sim 10^6$ $(cm^2\text{-sec})^{-1}$. Discussions of the salient features of the spatial distributions and the temporal variations of outer zone electron intensities evident in the contours of the above Figures 3 through 7 have been previously given by Frank, Van Allen and Hills [1964] and Frank [1965a, b, c]. Our present purpose is directed toward presenting the first comprehensive summary of observations with the Explorer 14 array of G.M. tubes for the entire ten months of available telemetry coverage.

V. SUMMARY

A comprehensive graphic summary of the entire ten months of observations of the distributions and temporal variations of electron ($E > 40$ keV, > 230 keV and > 1.6 MeV) omnidirectional intensities in the outer radiation zone with an array of G.M. tubes borne on Explorer 14 has been developed and is displayed in Figures 3, 4, 5, 6 and 7. A similar presentation of measurements of electron ($E > 500$ keV) intensities within the outer radiation zone over a smaller range of L-values and a shorter epoch has been presented by McIlwain [1966b]. Two restrictions limit the application of the methods employed here. The first restriction is imposed by the orbital period of the satellite. An accurate record of gross changes in the intensities of electrons ($E > 40$ keV) requires a sampling interval of $\lesssim 1$ day. Longer intervals can be used to record large-scale temporal variations in higher-energy electron intensities. The contours for the electron ($E > 230$ keV and $E > 1.6$ MeV) intensities would not have been substantially changed if the satellite's period had been as great as 3 days with the exclusion of the periods surrounding the onsets of geomagnetic storms. Secondly, the plane of the satellite's orbit should lie close to the geomagnetic plane to effectively apply the present B/B_o correction; the B/B_o coordinates of the observations

through the outer zone should be $\lesssim 20$. The B/B_o adjustment used here was not sufficient to accurately normalize measurements obtained at higher magnetic latitudes. Further it is noted that the B and L coordinates assigned to the observations of electron intensities throughout this present investigation are derived solely with surface measurements of the geomagnetic field [Jensen and Cain, 1962] and hence that adiabatic acceleration and relocation of the outer zone electrons due to variable extraterrestrial ring currents and magnetospheric boundary currents [cf McIlwain, 1966a] are reflected in the contours of Figures 3 through 7 along with the non-adiabatic fluctuations. The present organization of observations of outer zone electron intensities has been undertaken to provide a comprehensive, concise medium for future comparison of these measurements with related observations, satellite and ground-based, and in order to most effectively display the prominent features of the morphology of outer zone electron intensities.

ACKNOWLEDGEMENTS

This research was supported in part by the National Aeronautics and Space Administration under Grant NsG-233-62.

REFERENCES

Davis, L. R., Low energy trapped protons and electrons, in Proc. Plasma Space Sci. Symp., ed. by C. C. Chang and S. S. Huang, D. Reidel Publishing Co., Dordrecht-Holland, pp. 212-226, 1965.

Frank, L. A., A survey of electrons E > 40 keV beyond 5 earth radii with Explorer XIV, J. Geophys. Res., 70, 1593-1626, 1965a.

Frank, L. A., Inward radial diffusion of electrons of greater than 1.6 million electron volts in the outer radiation zone, J. Geophys. Res., 70, 3533-3540, 1965b.

Frank, L. A., On the local-time dependence of outer radiation zone electron (E > 1.6 MeV) intensities near the magnetic equator, J. Geophys. Res., 70, 4131-4138, 1965c.

Frank, L. A., J. A. Van Allen, and H. K. Hills, A study of charged particles in the earth's outer radiation zone with Explorer 14, J. Geophys. Res., 69, 2171-2191, 1964.

Frank, L. A., J. A. Van Allen, W. A. Whelpley, and J. D. Craven, Absolute intensities of geomagnetically trapped particles with Explorer 14, J. Geophys. Res., 68, 1573-1579, 1963.

Freden, S. C., J. B. Blake, and G. A. Paulikas, Spatial variation of the inner zone trapped proton spectrum, J. Geophys. Res., 70, 3113-3116, 1965.

Gabbe, J. D. and W. L. Brown, Some observations of the distributions of energetic protons in the earth's radiation belts between 1962 and 1964, in Radiation Trapped in the Earth's Magnetic Field, Ed. by B. M. McCormac, D. Reidel Publishing Co., Dordrecht-Holland, pp. 165-184, 1966.

Jensen, D. C. and J. C. Cain, An interim geomagnetic field (abstract), J. Geophys. Res., 67, 3568-3569, 1962.

McIlwain, C. E., The radiation belts, natural and artificial, Science, 142, No. 3590, 355-361, 1963.

McIlwain, C. E., Ring current effects on trapped particles, J. Geophys. Res., 71, 3623-3628, 1966a.

McIlwain, C. E., Processes acting upon outer zone electrons I. Adiabatic perturbations, UCSD Res. Rep. SP-66-5, 1966b.

Vette, James I., Models of the Trapped Radiation Environment, Vol. I: Inner zone protons and electrons, NASA SP-3024, 1966.

FIGURE CAPTIONS

Figure 1. Responses of the 213B G.M. tube as functions of B/B_o for L = 4.0 and 5.0 during October 1962. Consecutive measurements (inbound (●) and outbound (○)) for each orbit are connected with straight lines.

Figure 2. Comparison (from top to bottom) of raw observations of electron (E > 230 keV) omnidirectional intensities, observations normalized to B/B_o = 1.0, and observations adjusted with the calculated efficiency $\epsilon(n)$ and normalized to B/B_o = 1.0 for the period October through December 1962 at L = 4.2. Daily sum K_p are included as the profile appearing at the bottom of this presentation.

Figure 3. Contours of constant omnidirectional intensities of electrons (E > 40 keV, > 230 keV, and > 1.6 MeV) at the magnetic equator during October through November 1962.

Figure 4. Continuation of Figure 3 for the period December 1962 through January 1963.

Figure 5. Continuation of Figure 3 for the period February through March 1963.

Figure 6. Continuation of Figure 3 for the period April through May 1963.

Figure 7. Continuation of Figure 3 for the period June through July 1963.

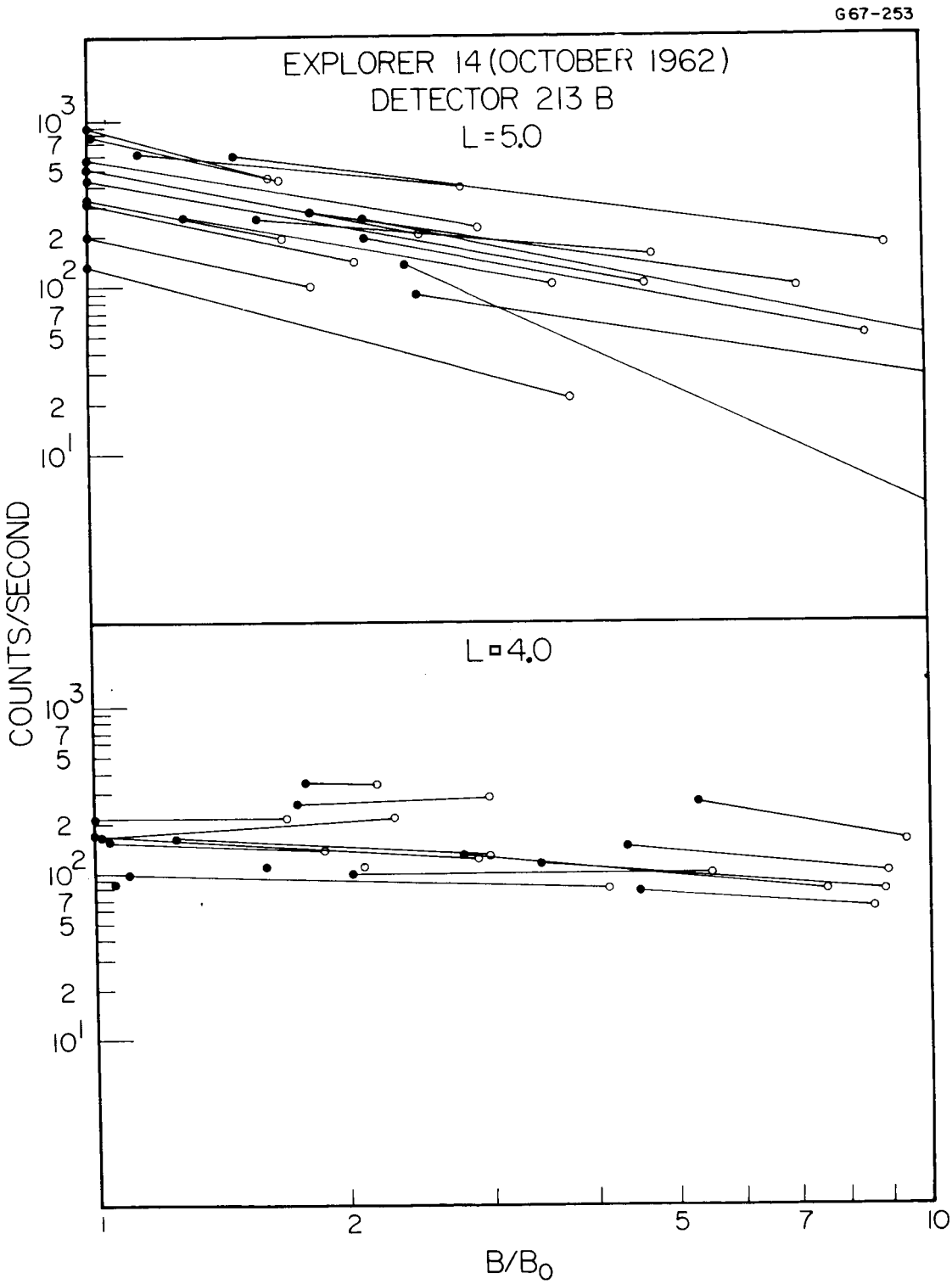
G67-253
EXPLORER 14 (OCTOBER 1962)
DETECTOR 213 B
L = 5.0
L = 4.0
COUNTS/SECOND
10^3
7
5
2
10^2
7
5
2
10^1
1
2
5
7
10
B/B_0

Figure 1

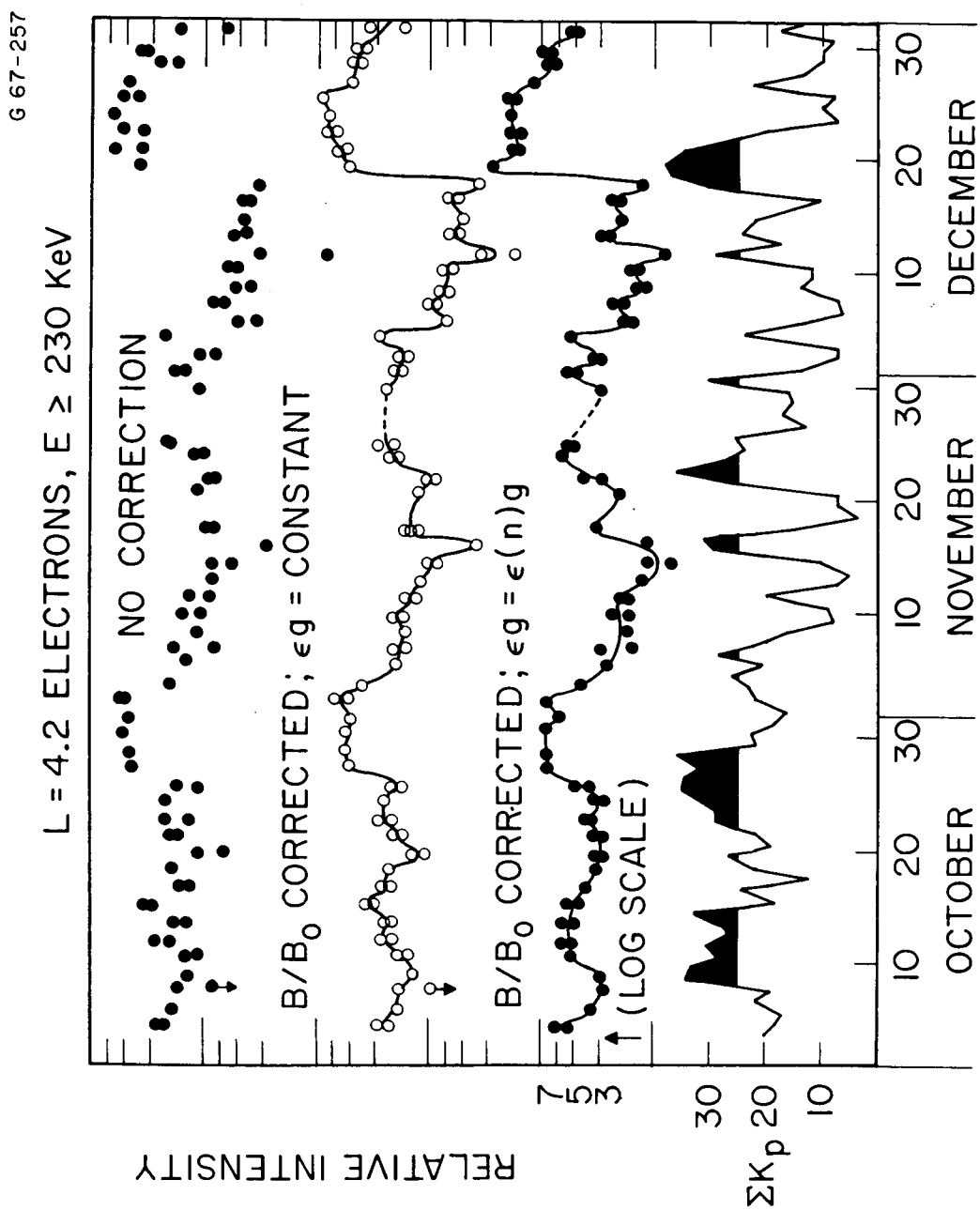
G 67-257
L = 4.2 ELECTRONS, E ≥ 230 KeV
NO CORRECTION
B/B0 CORRECTED; εg = CONSTANT
B/B0 CORRECTED; εg = ε(n)g
↑ (LOG SCALE)
RELATIVE INTENSITY
7
5
3
ΣKp
30
20
10
10
20
30
OCTOBER
10
20
30
NOVEMBER
10
20
30
DECEMBER
1962

Figure 2

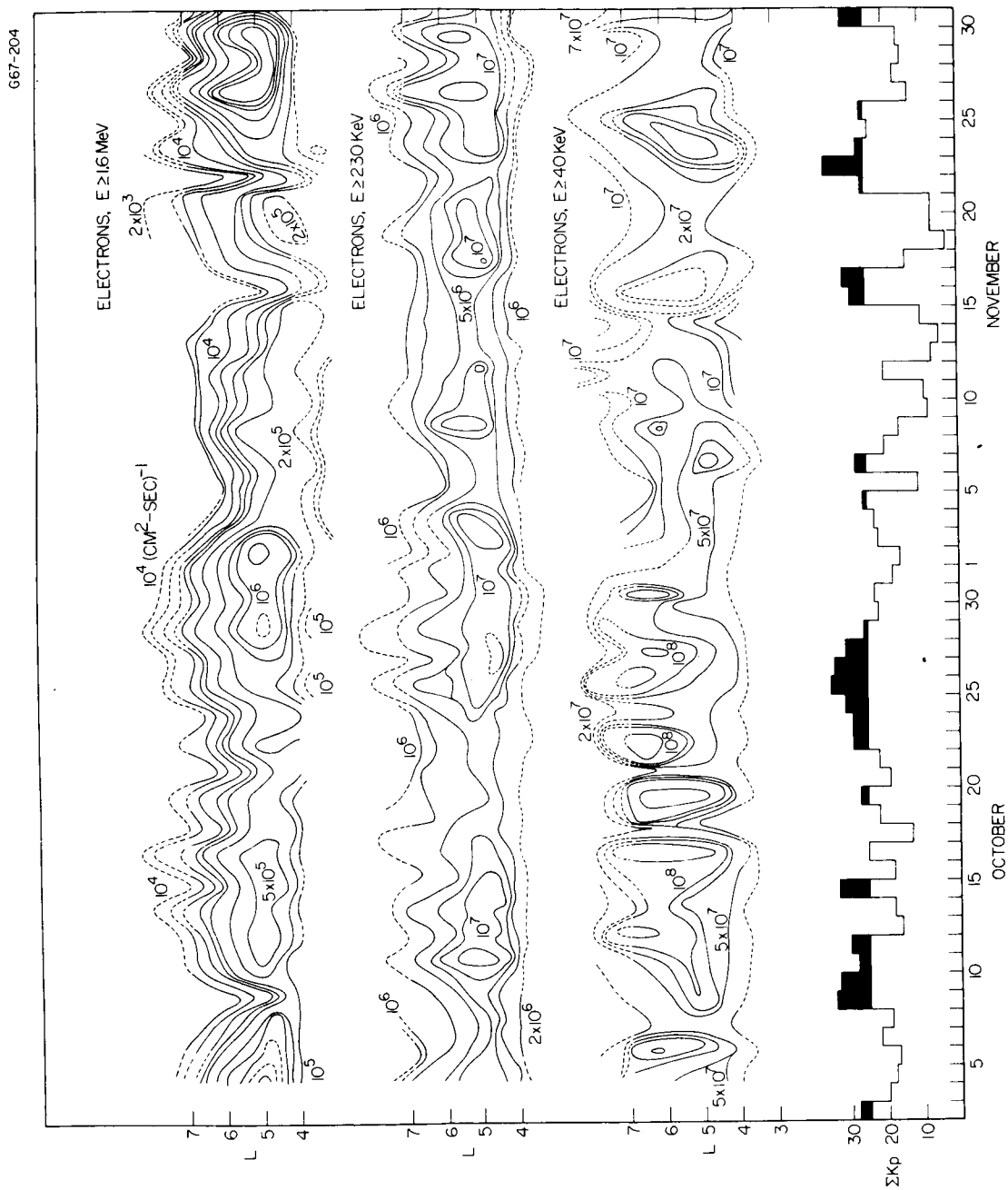
667-204
ELECTRONS, E ≥ 1.6 MeV
10^4 (CM^2-SEC)$^{-1}$
ELECTRONS, E ≥ 230 KeV
ELECTRONS, E ≥ 40 KeV
L
ΣKp
OCTOBER
NOVEMBER

Figure 3

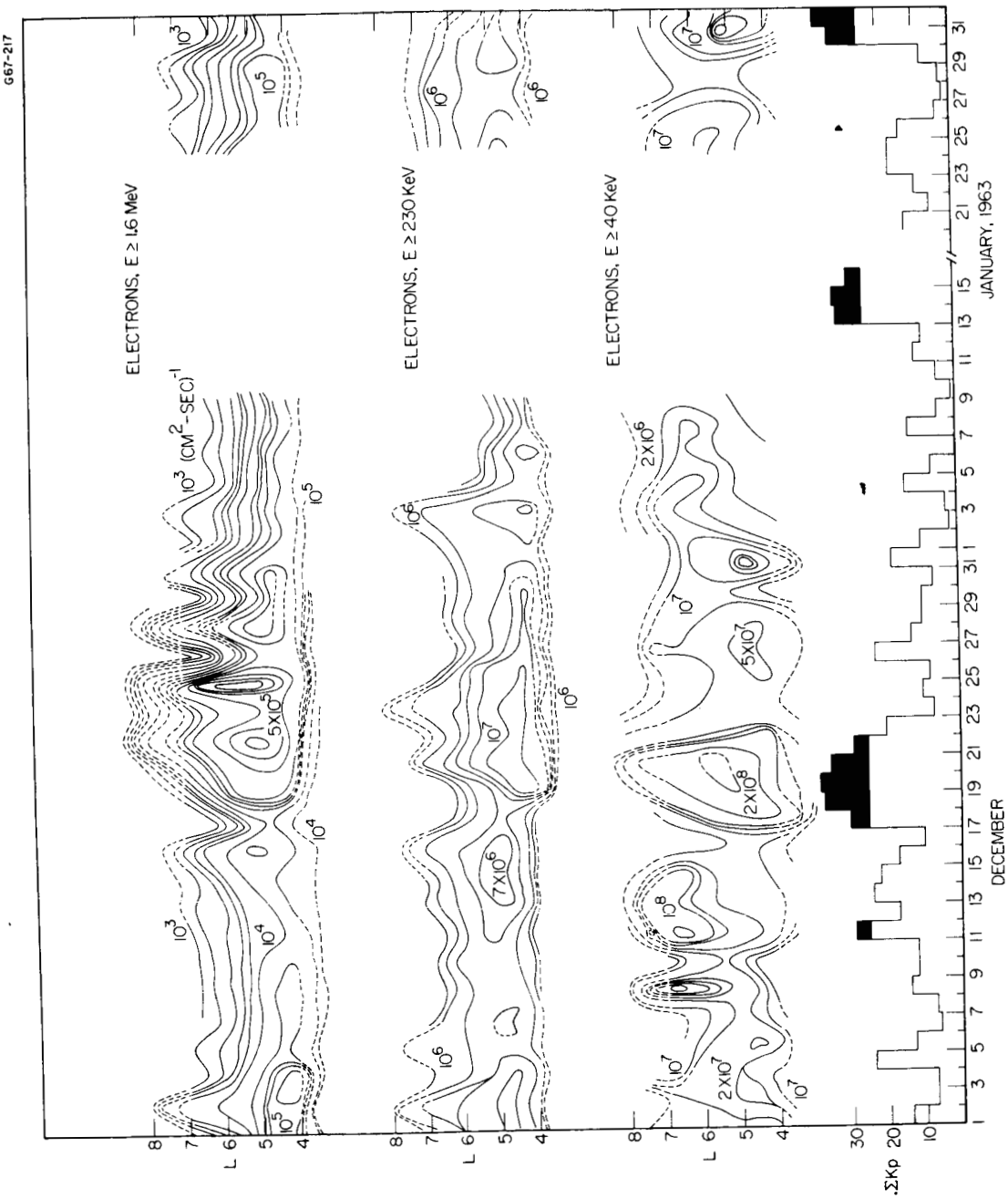
G67-217
ELECTRONS, E ≥ 1.6 MeV
ELECTRONS, E ≥ 230 KeV
ELECTRONS, E ≥ 40 KeV
10^3 (CM^2-SEC)$^{-1}$
L
ΣKp
DECEMBER
JANUARY, 1963

Figure 4

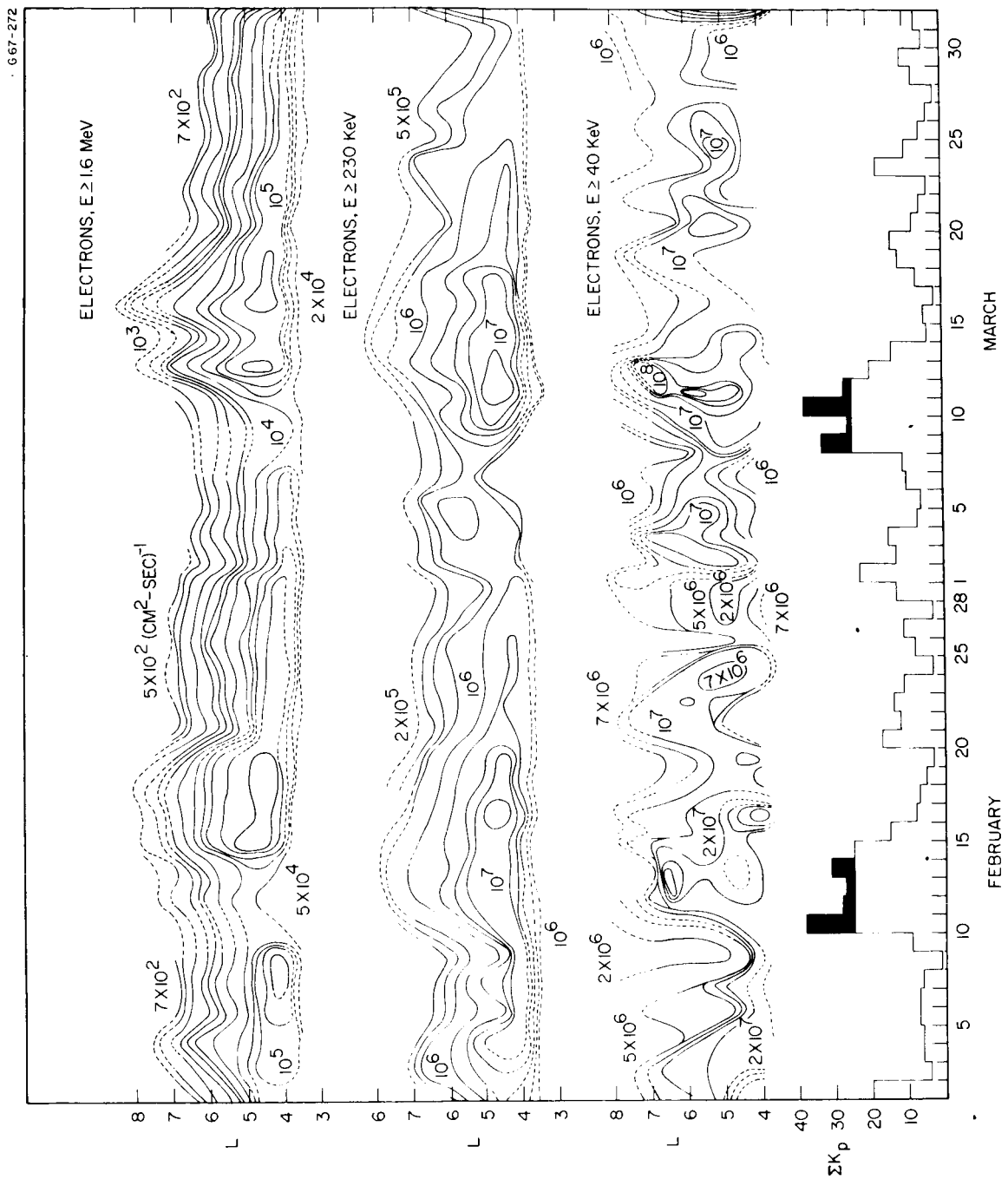
G67-272
ELECTRONS, E ≥ 1.6 MeV
ELECTRONS, E ≥ 230 KeV
ELECTRONS, E ≥ 40 KeV
5X10² (CM²-SEC)⁻¹
L
ΣKp
FEBRUARY
MARCH

Figure 5

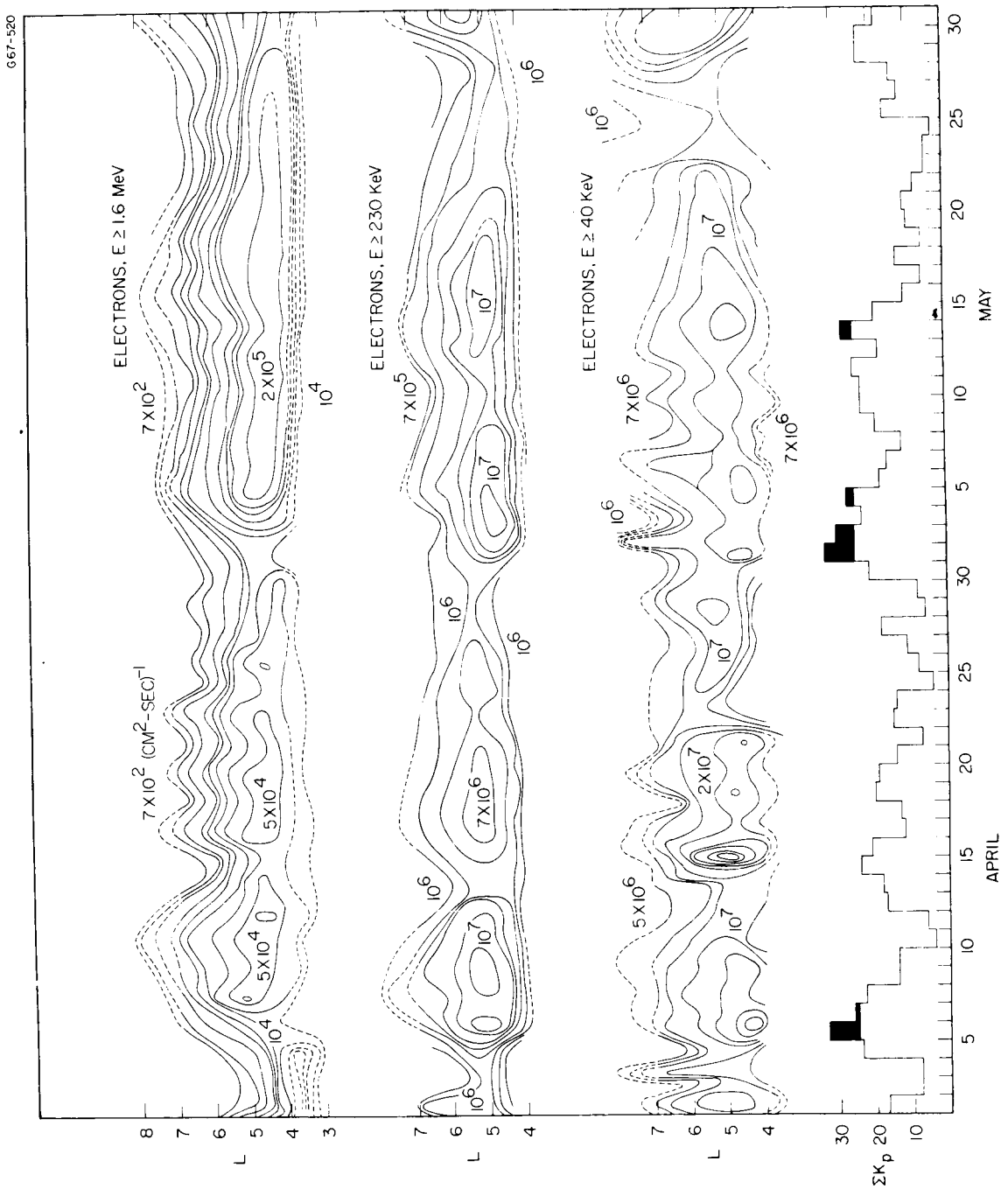
667-520
ELECTRONS, E ≥ 1.6 MeV
7X10² (CM²-SEC)⁻¹
7X10²
2X10⁵
10⁴
5X10⁴
ELECTRONS, E ≥ 230 KeV
7X10⁵
10⁷
10⁶
7X10⁶
ELECTRONS, E ≥ 40 KeV
7X10⁶
2X10⁷
5X10⁶
L
ΣKp
APRIL
MAY

Figure 6

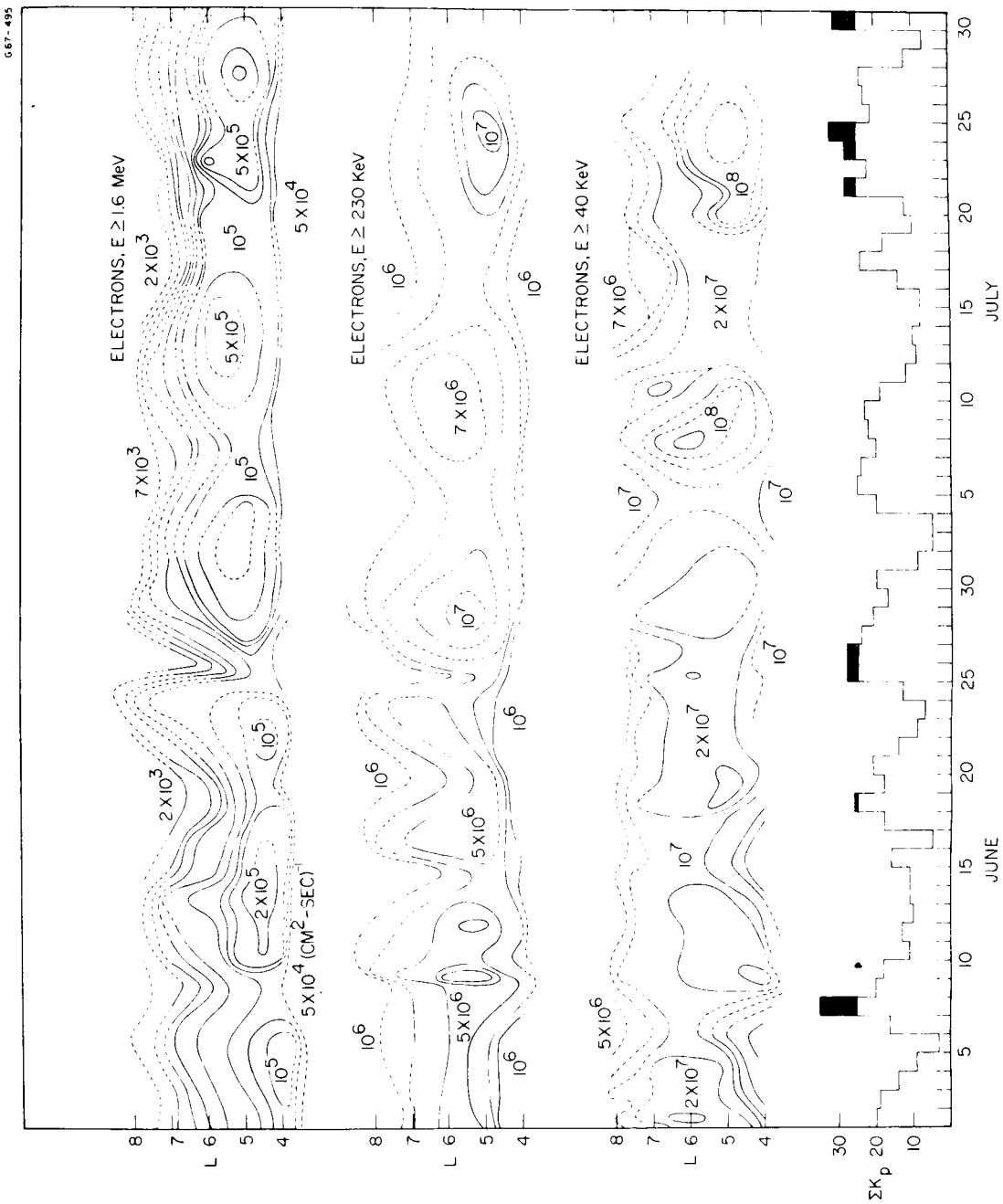
667-495
ELECTRONS, E ≥ 1.6 MeV
ELECTRONS, E ≥ 230 KeV
ELECTRONS, E ≥ 40 KeV
5X10⁴ (CM²-SEC)⁻¹
L
ΣKp
JUNE
JULY

Figure 7